Electric Power Systems Research 190 (2021) 106542

Contents lists available at ScienceDirect

Electric Power Systems Research

journal homepage: www.elsevier.com/locate/epsr

Balancibility: Existence and uniqueness of power flow solutions under voltage balance requirements☆

Bowen Li[a,*], Bai Cui[a], Feng Qiu[a], Daniel K. Molzahn[b]

[a] Energy Systems Division, Argonne National Laboratory, Lemont, IL, USA
[b] School of Electrical and Computer Engineering, Georgia Institute of Technology, Atlanta, GA, USA

ARTICLE INFO

Keywords:
Distribution network
Power flow solvability
Quadratically constrained quadratic program
Semidefinite programming
Voltage unbalance

ABSTRACT

In distribution systems, power injection variability due to growing penetrations of distributed energy resources (DERs) and dispatchable loads can lead to power quality issues such as severe voltage unbalance. To ensure safe operation of phase-balance-sensitive components such as three-phase motor loads, the amount of voltage unbalance must be maintained within specified limits for a range of uncertain loading conditions. This paper builds on existing "solvability conditions" that characterize operating regions for which the power flow equations are guaranteed to admit a unique high-voltage solution. We extend these existing solvability conditions to be applicable to distribution systems and augment them with a "balancibility" condition that quantifies an operating region within which a unique, adequately balanced power flow solution exists. To build this condition, we consider different unbalance definitions and derive closed-form representations through reformulations or safe approximations. Using case studies, we evaluate these closed-form representations and compare the balancibility conditions associated with different unbalance definitions.

1. Introduction

Increasing penetrations of distributed energy resources (DERs) and dispatchable loads can result in greater variability and stochasticity of the power injections in distribution systems. Extreme variations in power injections can also lead to power quality issues such as significant voltage unbalances. Unbalanced voltages can greatly impact essential power system devices such as three-phase induction motors and transformers [1,2]. Specifically, for induction motors, even small amounts of voltage unbalance can cause severe temperature rise, efficiency loss, and decreased life expectancy, which leads to serious consequences from premature motor failures, costly shutdowns, and lost production [3]. Voltage unbalance is estimated to cause annual losses to U.S. industries of up to $28 billion [4]. Hence, it is critical to provide secure criteria for power system operations subject to uncertainties (e.g., renewable generation and load consumption) such that the resulting operating points have voltage balance guarantees.

Organizations such as International Electrotechnical Commission (IEC), National Electrical Manufacturers Association (NEMA), and IEEE have each developed definitions to quantify the amount of voltage unbalance. For example, IEC [5] and IEEE [6] have definitions that are based on the ratio between negative/zero-sequence voltage and positive-sequence voltage calculated from the symmetrical component transformation. Other standards from NEMA [7] and IEEE [8,9] define voltage unbalance using line-to-line and line-to-ground voltage magnitudes, respectively. Previous research in [10] and [11] summarizes and compares these definitions.

This paper characterizes regions of power injections for which the power flow equations admit a unique high-voltage solution that satisfies specified phase unbalance requirements according to these definitions. This paper extends existing power flow solvability conditions, which have been extensively studied for both transmission systems [12–14] and distribution systems [15–18], in order to consider voltage balance requirements. This extension results in our proposed "balancibility" condition, which quantifies a region of power injections for which a unique and adequately balanced power flow solution is guaranteed to exist.

To the best of our knowledge, this is the first paper to incorporate voltage balance requirements into power flow solvability conditions. As specific contributions, we consider different unbalance definitions and develop various approaches for deriving closed-form representations or safe approximations that quantify the voltage unbalance level. We say a

☆ This work was funded by the U.S. Department of Energy's Office of Energy Efficiency and Renewable Energy (EERE) under Solar Energy Technologies Office (SETO) Agreement Number 34235.

* Corresponding author.
E-mail addresses: bowen.li@anl.gov (B. Li), bcui@anl.gov (B. Cui), fqiu@anl.gov (F. Qiu), molzahn@gatech.edu (D.K. Molzahn).

https://doi.org/10.1016/j.epsr.2020.106542
Received 10 October 2019; Received in revised form 7 April 2020; Accepted 19 July 2020
Available online 05 August 2020

set is a "safe approximation" of a robust set if it contains the entire robust set. We use a general model to describe the sets that contain the power flow solutions under uncertain power injections and provide supporting theoretical guarantees on the quality of the approaches. We demonstrate the proposed balancibility condition using the solvability condition in [14]. We then numerically illustrate the quality of the balancibility conditions associated with different unbalance definitions.

The proposed balancibility condition is expected to be a key enabling tool for many applications due to its ability to greatly simplify various problem formulations. One important application is reformulating the power flow equations in stochastic optimization problems in order to guarantee satisfaction of voltage balance requirements despite uncertain power injections. The balancibility condition can also be used to identify and ameliorate voltage unbalance problems at critical buses as well as to characterize worst-case uncertainty realizations with respect to voltage balance limits.

The remainder of the paper is organized as follows. Section 2 introduces notation. Section 3 describes the distribution network model and the solvability condition from Cui and Sun [14]. Section 4 derives the closed-form approximations or reformulations for various unbalance definitions and proposes our balancibility condition. Section 5 presents case studies. Section 6 summarizes the paper and discusses future directions.

2. Notation

Boldface letters indicate complex variables and roman font is used for real variables. The complex unit is $\boldsymbol{j} = \sqrt{-1}$. Transposition and Hermitian transposition are denoted as $(\cdot)^\top$ and $(\cdot)^{\mathrm{H}}$, respectively. $\mathbb{I}_n \in \mathbb{R}^{n\times n}$ represents the identity matrix. $\mathbb{O}_n$ denotes an $n \times n$ zero matrix. $\mathcal{H}^n$ denotes the set of $n \times n$ Hermitian matrices. For $y \in \mathbb{R}$, $\lfloor y \rfloor$ returns the greatest integer less than or equal to y. For $x \in \mathbb{R}^n$ or $\mathbb{C}^n$, $\bar{x}$ denotes its component-wise conjugate. $\mathrm{Re}(\boldsymbol{x})$ and $\mathrm{Im}(\boldsymbol{x})$ denote the component-wise real and imaginary parts, respectively, of x. x_i denotes the i-th entry in the vector x and $x_{i,j}$ $(i \le j)$ denotes the vector from i-th entry to j-th entry. $\|x\|$ denotes the ℓ_2-norm and $\|x\|_p$ denotes the ℓ_p-norm. $|\boldsymbol{x}|$ returns the magnitude of $\boldsymbol{x} \in \mathbb{C}$. All angle values are reported in degrees. $\mathcal{A} \times \mathcal{B}$ denotes the Cartesian product of sets $\mathcal{A}$ and $\mathcal{B}$. $\mathcal{A}^n$ represents the Cartesian product with set $\mathcal{A}$ for n times. For matrix $X \in \mathbb{C}^{n\times n}$ or $\mathbb{R}^{n\times n}$, X_{ij} represents the entry at i-th row and j-th column. X_i represents the vector of the i-th row. $X_i^{j,k}$ $(j \le k)$ represents the vector from j-th to k-th elements in the i-th row of X. $N(X)$ represents the nullspace of X. $\mathrm{rank}(X)$ and $\mathrm{Tr}(X)$ return the rank and trace, respectively, of X. $X \succeq 0$ indicates positive semidefiniteness of X. The function $\boldsymbol{\lambda}_{\min}(X)$ returns the smallest eigenvalue of X. The function $\mathrm{blkdiag}(\cdot)$ returns a block diagonal matrix with its input matrices and $\mathrm{diag}(\cdot)$ returns a diagonal matrix. $\mathbf{0}$ $(\mathbf{1})$ represents all-zero (all-one) vector or matrix with appropriate size. For a set S, its closure and boundary are denoted by $\bar{S}$ and ∂S, respectively. $D(x, r)$ represents an open disk with center x and radius r. For brevity, we denote $D(0, r)$ by $D(r)$.

3. Network model and solvability condition

In this paper, we use a distribution network model similar to [14,18] and assume a generic network topology (i.e., radial or meshed) with a single slack bus and multiple-phase wye-connected PQ buses.[1] We choose the slack bus to be at node 0 and define $\mathcal{N}_L$ as the set of PQ buses. Denote the voltage at the slack bus as $\mathbf{V}_G = (\mathbf{V}_{G,a}, \mathbf{V}_{G,b}, \mathbf{V}_{G,c})^\top$ for each phase a, b, c. Similarly, for all $i \in \mathcal{N}_L$, we define its wye-connected power consumption to be $\mathbf{S}_L^i = (\mathbf{S}_{L,a}^i, \mathbf{S}_{L,b}^i, \mathbf{S}_{L,a}^i)^\top$ and its voltage to be $\mathbf{V}_L^i = (\mathbf{V}_{L,a}^i, \mathbf{V}_{L,b}^i, \mathbf{V}_{L,a}^i)^\top$. Based on the admittance matrix $\mathbf{Y}$, we have

$$\begin{bmatrix} \mathbf{I}_G \\ -\mathbf{I}_L \end{bmatrix} = \begin{bmatrix} \mathbf{Y_{GG}} & \mathbf{Y_{GL}} \\ \mathbf{Y_{LG}} & \mathbf{Y_{LL}} \end{bmatrix} \begin{bmatrix} \mathbf{V}_G \\ -\mathbf{V}_L \end{bmatrix}, \tag{1}$$

where $\mathbf{I}_G$ is the current injected at the slack bus and $\mathbf{I}_L$ is the current withdrawn at PQ buses.[2] Based on [14,18], we have

$$\mathbf{v}_L = \mathbf{1} - \hat{\mathbf{Z}}\,\mathrm{diag}^{-1}(\bar{\mathbf{v}}_L)\bar{\mathbf{S}}_L, \tag{2}$$

where[3]

$$\mathbf{E} = -\mathbf{Y}_{LL}^{-1}\mathbf{Y}_{LG}\mathbf{V}_G, \tag{3a}$$

$$\mathbf{v}_L = \mathrm{diag}^{-1}(\mathbf{E})\,\mathbf{V}_L, \tag{3b}$$

$$\hat{\mathbf{Z}} = \mathrm{diag}^{-1}(\mathbf{E})\,\mathbf{Y}_{LL}^{-1}\,\mathrm{diag}^{-1}(\bar{\mathbf{E}}). \tag{3c}$$

We use the solvability condition from [14] to analyze the secure region of $\mathbf{S}_L$ for which there exists a unique $\mathbf{V}_L$ within a set $\mathcal{V}_L(\mathbf{S}_L)$ (i.e., parameterized on $\mathbf{S}_L$). As illustrated in Fig. 1, if $\mathbf{S}_L$ changes in its uncertainty set, $\mathcal{V}_L$ also changes to follow the power flow solution $\mathbf{V}_L$ if the solvability condition is satisfied. The uncertainty set of $\mathbf{S}_L$ is typically constructed using historical data and we do not assume any specific structure for this set. In practice, any computationally efficient selection of this set will suffice. Since the variation of $\mathcal{V}_L$ can be easily represented as an explicit function of $\mathbf{S}_L$, the solvability condition summarized in this section provides an efficient way to confidently locate the power flow solution under uncertainty. A detailed description of this condition is available in [14].

Define a nominal power flow solution $(\mathbf{v}_L^0, \mathbf{S}_L^0)$,

$$\mathbf{v}_L^0 = \mathbf{1} - \hat{\mathbf{Z}}\,\mathrm{diag}^{-1}(\bar{\mathbf{v}}_L^0)\,\bar{\mathbf{S}}_L^0, \tag{4}$$

and $\boldsymbol{\sigma}_L = \mathbf{S}_L - \mathbf{S}_L^0$. If no nominal solution is provided, a trivial selection is $\mathbf{v}_L^0 = \mathbf{1}$ when $\mathbf{S}_L^0 = 0$. We also define the following quantities used in the solvability condition and $\mathcal{V}_L$:

$$\tilde{\mathbf{Z}} = \mathrm{diag}^{-1}(\mathbf{v}_L^0)\,\hat{\mathbf{Z}}\,\mathrm{diag}^{-1}(\bar{\mathbf{v}}_L^0), \quad \mathbf{u}_L = \mathrm{diag}^{-1}(\mathbf{v}_L^0)\,\mathbf{v}_L.$$

For $i \in \mathcal{N}_L$ and phase $p \in \{a, b, c\}$, denote $\tilde{\mathbf{Z}}_i^p$ as the corresponding row of $\tilde{\mathbf{Z}}$ and define

$$\eta_{i,p}(\boldsymbol{\sigma}_L) = (\tilde{\mathbf{Z}}_i^p)^\top \bar{\boldsymbol{\sigma}}_L, \quad \xi_{i,p}(\mathbf{S}_L) = \|(\tilde{\mathbf{Z}}_i^p)^\top \mathrm{diag}(\bar{\mathbf{S}}_L)\|_1,$$
$$\gamma_{i,p}(\boldsymbol{\sigma}_L, \mathbf{S}_L) = 2(\xi_{i,p}(\mathbf{S}_L) + \mathrm{Re}(\eta_{i,p}(\boldsymbol{\sigma}_L))) - |\eta_{i,p}(\boldsymbol{\sigma}_L)|^2 - \xi_{i,p}(\mathbf{S}_L)^2,$$

where $\eta_{i,p}(\boldsymbol{\sigma}_L)$ and $\xi_{i,p}(\mathbf{S}_L)$ represent aggregated system stress measures on each node and phase resulting from incremental and total loads. These measures appear in other existing solvability literature [13,16,19]. We also define $\gamma_{i,p}(\boldsymbol{\sigma}_L, \mathbf{S}_L)$ fusing these two stresses. Accordingly, we define

$$\eta(\boldsymbol{\sigma}_L) = \max_{i\in\mathcal{N}_L,\ p\in\{a,b,c\}} |\eta_{i,p}(\boldsymbol{\sigma}_L)|,$$
$$\xi(\mathbf{S}_L) = \max_{i\in\mathcal{N}_L,\ p\in\{a,b,c\}} \xi_{i,p}(\mathbf{S}_L),$$
$$\gamma(\boldsymbol{\sigma}_L, \mathbf{S}_L) = \max_{i\in\mathcal{N}_L,\ p\in\{a,b,c\}} \gamma_{i,p}(\boldsymbol{\sigma}_L, \mathbf{S}_L),$$
$$\Delta = (1 - \gamma(\boldsymbol{\sigma}_L, \mathbf{S}_L))^2 - 4\xi(\mathbf{S}_L)^2\eta(\boldsymbol{\sigma}_L)^2.$$

Next, we construct the following framework which geometrically quantifies a disk for $\mathbf{u}_L$ with parameter $r \ge 0$. For $i \in \mathcal{N}_L$ and $p \in \{a, b, c\}$, we have

$$\xi_{i,p}(\mathbf{S}_L) > 0: \quad |1 - \eta_{i,p}(\boldsymbol{\sigma}_L) - \mathbf{u}_{L,p}^i| \le r\,\xi_{i,p}(\mathbf{S}_L), \tag{5a}$$

$$\xi_{i,p}(\mathbf{S}_L) = 0: \quad \mathbf{u}_{L,p}^i = 1 - \eta_{i,p}(\boldsymbol{\sigma}_L). \tag{5b}$$

[1] The wye connection assumption comes from the solvability condition that we consider. However, the idea of the balancibility condition applies to other solvability conditions with different network assumptions (see Section 4).

[2] For two-phase or single-phase nodes, $\mathbf{V}_L$, $\mathbf{S}_L$, and $\mathbf{Y}$ only collect quantities for the existing phases.

[3] The invertibility of $\mathbf{Y}_{LL}$ is proved in [16]. As in [14,16,18], we assume that $\mathbf{E}$ and $\mathbf{v}_L$ do not contain zero elements, which is the case for practical power systems.

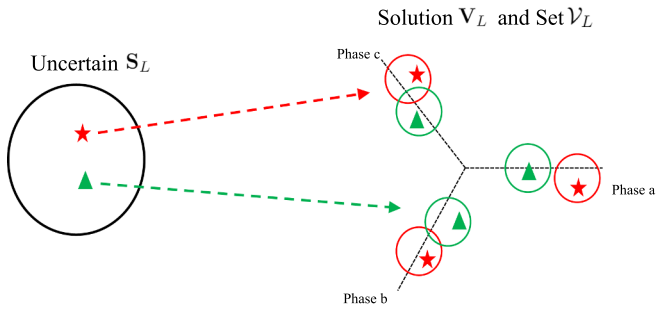

Fig. 1. Relationship among $\mathbf{S}_L$, $\mathbf{V}_L$, and $\mathcal{V}_L$.

Hence, when $\xi_{i,p}(\mathbf{S}_L) = 0$, $\mathbf{u}^i_{L,p}$ degenerates into a single point. The relationship between r and these quantities is presented in the next theorem.

Theorem 3.1. *(Theorem B.3 in [14]) Given a nominal solution* $(\mathbf{v}^0_L, \mathbf{S}^0_L)$*, if the following condition is satisfied*

$$\gamma(\sigma_L, \mathbf{S}_L) + 2\xi(\mathbf{S}_L)\eta(\sigma_L) < 1, \tag{6a}$$

$$\xi(\mathbf{S}_L) - \eta(\sigma_L) \le 1, \tag{6b}$$

then there exists a unique solution $\mathbf{u}_L$ *in (5) with*

$$\begin{cases} r = \sqrt{\frac{1-\gamma(\sigma_L,\mathbf{S}_L)-\sqrt{\Delta}}{2\xi(\mathbf{S}_L)^2}}, & \text{if } \xi(\mathbf{S}_L) > 0, \\ r = 0, & \text{if } \xi(\mathbf{S}_L) = 0. \end{cases} \tag{7}$$

From Theorem 3.1, we know where $\mathbf{u}_L$ is located under $\mathbf{S}_L$, which can then be used to obtain $\mathcal{V}_L$. For any $i \in \mathcal{N}_L$ and $p = \{a, b, c\}$, we have $\mathbf{V}^i_{L,p} = \mathbf{E}^i_p \mathbf{v}^{0,i}_{L,p} \mathbf{u}^i_{L,p}$ where $\mathbf{E}^i_p$ and $\mathbf{v}^{0,i}_{L,p}$ are corresponding terms in $\mathbf{E}$ and $\mathbf{v}^0_L$. Then, the set $\mathcal{V}^i_{L,p}$ that contains $\mathbf{V}^i_{L,p}$ can be represented as

$$|(1-\eta_{i,p}(\sigma_L))\mathbf{E}^i_p \mathbf{v}^{0,i}_{L,p} - \mathbf{V}^i_{L,p}| \le r|\mathbf{E}^i_p \mathbf{v}^{0,i}_{L,p}|\xi_{i,p}(\mathbf{S}_L). \tag{8}$$

With $\mathcal{V}_L$, we then have the foundations to analyze voltage unbalance levels under $(\mathbf{V}_L, \mathbf{S}_L)$ under uncertainty and derive balancibility conditions that limit this level.

4. Safe approximation on balancibility

This section derives our proposed the balancibility conditions which guarantee satisfaction of the voltage balance requirements for all the realizations in $\mathcal{V}_L$. We use safe approximations and different reformulation techniques to develop closed-form representations of these conditions. We choose safe approximations since relaxations may underestimate the true voltage unbalance level and give insecure results. We assume that there are critical nodes ($i^* \in \mathcal{N}_L$) that are sensitive to amounts of voltage unbalance outside of specified limits. Then, for each critical node, we rewrite $\mathcal{V}_L$ as a general set $\mathbf{U}_{in}$ (with $\mathbf{U}^p_{in}$ denoting a particular phase $p = \{a, b, c\}$) as

$$|\mathbf{V}_a - \mathbf{C}_a| \le r_a, \ |\mathbf{V}_b - \mathbf{C}_b| \le r_b, \ |\mathbf{V}_c - \mathbf{C}_c| \le r_c \tag{9}$$

where subscripts *a, b, c* denote the phases. Geometrically, $\mathbf{U}^p_{in}$ is a disk $\bar{D}(\mathbf{C}_p, r_p)$ with center $\mathbf{C}_p$ and radius r_p. To help some of the derivations, we also represent these sets in real coordinates, denoted $\mathcal{V}_{in}$, by separating the real and imaginary parts in (9):

$$(V^r_a - C^r_a)^2 + (V^i_a - C^i_a)^2 \le r_a^2, \tag{10a}$$

$$(V^r_b - C^r_b)^2 + (V^i_b - C^i_b)^2 \le r_b^2, \tag{10b}$$

$$(V^r_c - C^r_c)^2 + (V^i_c - C^i_c)^2 \le r_c^2, \tag{10c}$$

where the superscripts *r* and *i* denote the real and imaginary parts. Note that $\mathbf{U}_{in}/\mathcal{V}_{in}$ can be seen as a general output from any solvability conditions in complex domain [16–18] or involving voltage magnitudes [13]. Hence, the applicability is not restricted to any network assumptions (e.g., radial or wye-connected loads) or particular solvability condition [14].

Linking back to solvability condition (8) (taking phase *a* as an example), V^r_a and V^i_a represent the real and imaginary parts of the complex voltage $\mathbf{V}_a = \mathbf{V}^{i^*}_{L,a}$. C^r_a and C^i_a represent the real and imaginary parts of $\mathbf{C}_a = \left(1 - \eta_{i^*,a}(\sigma_L)\right)\mathbf{E}^{i^*}_a \mathbf{v}^{0,i^*}_{L,a}$ and $r_a = r|\mathbf{E}^{i^*}_a \mathbf{v}^{0,i^*}_{L,a}|\xi_{i^*,a}(\mathbf{S}_L)$. If $\xi_{i^*,a}(\mathbf{S}_L) = 0$, (5) is degenerate and V^r_a and V^i_a can be treated as constants while analyzing the voltage unbalance and hence do not affect the results.

To make (10) concise, we define vectors $V_a = (V^r_a, V^i_a)^\top \in \mathbb{R}^2$, $C_a = (C^r_a, C^i_a)^\top \in \mathbb{R}^2$, and set $\mathcal{V}^a_{in} \subset \mathbb{R}^2$: $=\{V_a$ that satisfies $(10a)\}$, with the same notations applied to phase *b* and *c*. We also define $V_{abc} = (V^\top_a, V^\top_b, V^\top_c)^\top \in \mathbb{R}^6$, $\mathbf{V}_{abc} = (\mathbf{V}_a, \mathbf{V}_b, \mathbf{V}_c)^\top \in \mathbb{C}^3$, $r_{abc} = (r_a, r_b, r_c)^\top \in \mathbb{R}^3_+$, and $C_{abc} = (C^\top_a, C^\top_b, C^\top_c)^\top \in \mathbb{R}^6$. Next, we derive the reformulations or safe approximations of the voltage balance requirement for different unbalance definitions.

4.1. Phase voltage unbalance rate (PVUR) definition

In [8], the following definition of phase voltage unbalance rate (*PVUR*) is provided using the line-to-ground voltage magnitudes $|\mathbf{V}_a|$, $|\mathbf{V}_b|$, and $|\mathbf{V}_c|$:

$$PVUR = \Delta^{\max}_V / V_{\text{avg}}, \tag{11}$$

where $V_{\text{avg}} = \frac{|\mathbf{V}_a|+|\mathbf{V}_b|+|\mathbf{V}_c|}{3}$ and

$\Delta^{\max}_V = \max\{||\mathbf{V}_a|-V_{\text{avg}}|, \ ||\mathbf{V}_b|-V_{\text{avg}}|, \ ||\mathbf{V}_c|-V_{\text{avg}}|\}$.

To ensure the power flow solutions are balanced, we require that the voltage profile satisfies (11) with a predefined tolerance of $\epsilon \in (0, 1)$ with $PVUR \le \epsilon$. This requirement is equivalent to the following linear constraints [20]:

$$\begin{bmatrix} \epsilon+2 & \epsilon-1 & \epsilon-1 \\ \epsilon-1 & \epsilon+2 & \epsilon-1 \\ \epsilon-1 & \epsilon-1 & \epsilon+2 \\ \epsilon-2 & \epsilon+1 & \epsilon+1 \\ \epsilon+1 & \epsilon-2 & \epsilon+1 \\ \epsilon+1 & \epsilon+1 & \epsilon-2 \end{bmatrix} \begin{bmatrix} |\mathbf{V}_a| \\ |\mathbf{V}_b| \\ |\mathbf{V}_c| \end{bmatrix} \ge \mathbf{0}. \tag{12}$$

Next, we require that all the solutions $V_{abc} \in \mathcal{V}_{in}$ satisfy (12). Without loss of generality, we only use the first linear constraint in (12) as an example and the problem becomes

$$\min_{V_{abc} \in \mathcal{V}_{in}} \{(\epsilon+2)|\mathbf{V}_a| + (\epsilon-1)|\mathbf{V}_b| + (\epsilon-1)|\mathbf{V}_c|\} \ge 0. \tag{13}$$

Since $\mathcal{V}_{in}$ is separable in each phase, (13) is equivalent to

$$\min_{V_a \in \mathcal{V}^a_{in}} (\epsilon+2)|\mathbf{V}_a| + \min_{V_b \in \mathcal{V}^b_{in}} (\epsilon-1)|\mathbf{V}_b| + \min_{V_c \in \mathcal{V}^c_{in}} (\epsilon-1)|\mathbf{V}_c| \ge 0. \tag{14}$$

Each subproblem in (14) can be easily solved since $\mathcal{V}^a_{in}$, $\mathcal{V}^b_{in}$, and $\mathcal{V}^c_{in}$ are closed disks. Since $\epsilon + 2 > 0$ and $\epsilon - 1 < 0$ ($\epsilon \in (0, 1)$), we have the following reformulation of (14):

$$(\epsilon+2)\max\{||C_a|| - r_a, 0\} + (\epsilon-1)(r_b + ||C_b||) \tag{15}$$

$$+ (\epsilon-1)(r_c + ||C_c||) \ge 0. \tag{16}$$

We use $\max\{||C_a|| - r_a, 0\}$ in case $|\mathbf{V}_a| = 0$ when $\mathcal{V}^a_{in}$ contains the origin. Now, we can derive the voltage balance requirements using each of the linear constraints in (12). This approach also applies to other *PVUR* definitions as in [9,10] where

$\Delta^{\max}_V = \max\{|\mathbf{V}_a|, |\mathbf{V}_b|, |\mathbf{V}_c|\} - \min\{|\mathbf{V}_a|, |\mathbf{V}_b|, |\mathbf{V}_c|\}$.

4.2. Line voltage unbalance rate (LVUR) definition

In [7], an unbalance definition called the line voltage unbalance rate (*LVUR*) is provided using line-to-line voltages $|\mathbf{V}_{ab}| = |\mathbf{V}_a - \mathbf{V}_b|$, $|\mathbf{V}_{bc}| = |\mathbf{V}_b - \mathbf{V}_c|$, and $|\mathbf{V}_{ca}| = |\mathbf{V}_c - \mathbf{V}_a|$:

$$LVUR = \Delta_{V_L}^{\max}/V_{\text{avg},L}, \tag{17}$$

where $V_{\text{avg},L} = \frac{|\mathbf{V}_{ab}|+|\mathbf{V}_{bc}|+|\mathbf{V}_{ca}|}{3}$ and

$\Delta_{V_L}^{max} = \max\{||\mathbf{V}_{ab}|-V_{\text{avg}}|,\ ||\mathbf{V}_{bc}|-V_{\text{avg}}|,\ ||\mathbf{V}_{ca}|-V_{\text{avg}}|\}$.

Similar to *PVUR*, with voltage balance requirement $LVUR \le \epsilon$, we have

$$\begin{bmatrix} \epsilon+2 & \epsilon-1 & \epsilon-1 \\ \epsilon-1 & \epsilon+2 & \epsilon-1 \\ \epsilon-1 & \epsilon-1 & \epsilon+2 \\ \epsilon-2 & \epsilon+1 & \epsilon+1 \\ \epsilon+1 & \epsilon-2 & \epsilon+1 \\ \epsilon+1 & \epsilon+1 & \epsilon-2 \end{bmatrix} \begin{bmatrix} |\mathbf{V}_{ab}| \\ |\mathbf{V}_{bc}| \\ |\mathbf{V}_{ca}| \end{bmatrix} \ge \mathbf{0}. \tag{18}$$

We require that all $V_{abc} \in \mathcal{V}_{in}$ satisfy (18). Here, we use the first constraint in (18) as an example:

$$\left\{ \min_{V_{abc}\in\mathcal{V}_{in}} (\epsilon+2)|\mathbf{V}_{ab}| + (\epsilon-1)|\mathbf{V}_{bc}| + (\epsilon-1)|\mathbf{V}_{ca}| \right\} \ge 0. \tag{19}$$

There are several approaches for safely approximating (19). The first approach bounds $|\mathbf{V}_{ab}|$, $|\mathbf{V}_{bc}|$, and $|\mathbf{V}_{ca}|$ as in [21]. Taking $|\mathbf{V}_{ab}|$ as an example, we have

$$|\mathbf{V}_{ab}| = ||C_a - C_b + r_a u_a + r_b u_b||$$

where u_a and u_b are any vectors in the unit ball in $\mathbb{R}^2$. Then, we see that

$$\max\{||C_a - C_b|| - r_a - r_b, 0\} \le |\mathbf{V}_{ab}|, \tag{20a}$$

$$||C_a - C_b|| + r_a + r_b \ge |\mathbf{V}_{ab}|. \tag{20b}$$

The voltages $|\mathbf{V}_{bc}|$ and $|\mathbf{V}_{ca}|$ are bounded analogously. Using a similar idea as in (14), we safely approximate (19) as

$$\begin{aligned} &(\epsilon+2)\max\{||C_a - C_b|| - r_a - r_b, 0\} \\ &\quad + (\epsilon-1)(||C_b - C_c|| + r_b + r_c) \\ &\quad + (\epsilon-1)(||C_a - C_b|| + r_b + r_c) \ge 0. \end{aligned} \tag{21}$$

The second approach for approximating (19) uses the following relationship:

$$\begin{aligned} &||\mathbf{V}_a| - |\mathbf{V}_b|| \le |\mathbf{V}_{ab}| \le |\mathbf{V}_a| + |\mathbf{V}_b|, \\ &||\mathbf{V}_b| - |\mathbf{V}_c|| \le |\mathbf{V}_{bc}| \le |\mathbf{V}_b| + |\mathbf{V}_c|, \\ &||\mathbf{V}_c| - |\mathbf{V}_a|| \le |\mathbf{V}_{ca}| \le |\mathbf{V}_c| + |\mathbf{V}_a|. \end{aligned}$$

Denote $|\mathbf{V}_{abc}| = (|\mathbf{V}_a|, |\mathbf{V}_b|, |\mathbf{V}_c|)^\top$. Since $\epsilon \in (0, 1)$, we also have

$$\begin{aligned} &\min_{V_{abc}\in\mathcal{V}_{in}} (\epsilon+2)|\mathbf{V}_{ab}| + (\epsilon-1)|\mathbf{V}_{bc}| + (\epsilon-1)|\mathbf{V}_{ca}| \\ &\ge \min_{V_{abc}\in\mathcal{V}_{in}} (\epsilon+2)||\mathbf{V}_a| - |\mathbf{V}_b|| + (\epsilon-1)(|\mathbf{V}_b| + |\mathbf{V}_c|) \\ &\qquad + (\epsilon-1)(|\mathbf{V}_c| + |\mathbf{V}_a|) \\ &= \min_{Q|\mathbf{V}_{abc}|\le q} (\epsilon+2)||\mathbf{V}_a| - |\mathbf{V}_b|| + (\epsilon-1)(|\mathbf{V}_b| + |\mathbf{V}_c|) \\ &\qquad + (\epsilon-1)(|\mathbf{V}_c| + |\mathbf{V}_a|) \end{aligned} \tag{22}$$

where $Q = [\mathbb{I}_3, -\mathbb{I}_3]^\top$ and

$$\begin{aligned} q = \ &(r_a+||C_a||, r_b+||C_b||, r_c+||C_c||, \min\{r_a-||C_a||, 0\}, \\ &\min\{r_b-||C_b||, 0\}, \min\{r_c-||C_c||, 0\})^\top. \end{aligned}$$

The last equality in (22) is true since V_{abc} is independent in each phase in $\mathcal{V}_{in}$, Similar to (14), only the upper and lower bounds of $|\mathbf{V}_{abc}|$ are taking effect. It can be seen that (22) is convex and the feasible set $Q|\mathbf{V}_{abc}| \le q$ only has eight extreme points (combinations of upper and lower bounds for $|\mathbf{V}_{abc}|$. Hence, evaluating the extreme points and finding the minimum efficiently solves (22). Linear program duality [22] can also be used to handle (22). Below, we directly give the duality-based safe approximation to (19) by introducing the dual variable λ:

$$-\hat{q}^\top\lambda \ge 0,\ \ \hat{Q}^\top\lambda + c = 0,\ \ \lambda \ge 0,$$

where $\hat{q} = (q^\top, 0, 0)^\top$, $c = (\epsilon-1, \epsilon-1, 2\epsilon-2, \epsilon+2)^\top$, and

$$\hat{Q} = \begin{bmatrix} & Q & & \mathbf{0} \\ 1 & -1 & 0 & -1 \\ -1 & 1 & 0 & -1 \end{bmatrix}.$$

4.3. Voltage unbalance factor (VUF) definition

References [5] and [6] give the following voltage unbalance factor (*VUF*) definitions based on the magnitudes of negative-, positive-, and zero-sequence voltages, $\mathbf{V}_n$, $\mathbf{V}_p$, and $\mathbf{V}_0$, respectively:

$$VUF_n = |\mathbf{V}_n|/|\mathbf{V}_p|, \tag{23a}$$

$$VUF_0 = |\mathbf{V}_0|/|\mathbf{V}_p|, \tag{23b}$$

where

$$\mathbf{V}_p = (\mathbf{V}_a + \alpha\mathbf{V}_b + \alpha^2\mathbf{V}_c)/3, \tag{24a}$$

$$\mathbf{V}_n = (\mathbf{V}_a + \alpha^2\mathbf{V}_b + \alpha\mathbf{V}_c)/3, \tag{24b}$$

$$\mathbf{V}_0 = (\mathbf{V}_a + \mathbf{V}_b + \mathbf{V}_c)/3, \tag{24c}$$

and $\alpha = 1\angle 120°$. With the tolerance $\epsilon \in (0, 1)$, we equivalently transform the voltage balance requirements into quadratic inequality constraints:

$$|\mathbf{V}_n|/|\mathbf{V}_p| \le \epsilon \ \Leftrightarrow\ \mathbf{V}_n\bar{\mathbf{V}}_n - \epsilon^2\mathbf{V}_p\bar{\mathbf{V}}_p \le 0, \tag{25a}$$

$$|\mathbf{V}_0|/|\mathbf{V}_p| \le \epsilon \ \Leftrightarrow\ \mathbf{V}_0\bar{\mathbf{V}}_0 - \epsilon^2\mathbf{V}_p\bar{\mathbf{V}}_p \le 0. \tag{25b}$$

Next, to ensure the power flow solutions are balanced, we obtain the following constraints

$$\left\{ \max_{\mathbf{V}_{abc}\in\mathbf{U}_{in}} \mathbf{V}_n\bar{\mathbf{V}}_n - \epsilon^2\mathbf{V}_p\bar{\mathbf{V}}_p \right\} \le 0, \tag{26a}$$

$$\left\{ \max_{\mathbf{V}_{abc}\in\mathbf{U}_{in}} \mathbf{V}_0\bar{\mathbf{V}}_0 - \epsilon^2\mathbf{V}_p\bar{\mathbf{V}}_p \right\} \le 0. \tag{26b}$$

A direct way to safely approximate (26) is using approximation by bound. For example, (26a) is implied by

$$\left\{ \max_{\mathbf{V}_{abc}\in\mathbf{U}_{in}} 9\mathbf{V}_n\bar{\mathbf{V}}_n - \epsilon^2 \min_{\mathbf{V}_{abc}\in\mathbf{U}_{in}} 9\mathbf{V}_p\bar{\mathbf{V}}_p \right\} \le 0 \tag{27}$$

where scaling helps eliminate 1/3 in (24). Further, we have

$$\max_{\mathbf{V}_{abc}\in\mathbf{U}_{in}} 9\mathbf{V}_n\bar{\mathbf{V}}_n \le (|\mathbf{C}_a + \alpha^2\mathbf{C}_b + \alpha\mathbf{C}_c| + r_a + r_b + r_c)^2$$

and the inequality is tight when $\mathbf{V}_a - \mathbf{C}_a$, $\alpha^2(\mathbf{V}_b - \mathbf{C}_b)$, and $\alpha(\mathbf{V}_c - \mathbf{C}_c)$ share the same angle as $\mathbf{C}_a + \alpha^2\mathbf{C}_b + \alpha\mathbf{C}_c$. Similarly, we get

$$\begin{aligned} &\min_{\mathbf{V}_{abc}\in\mathbf{U}_{in}} 9\mathbf{V}_p\bar{\mathbf{V}}_p \\ &\quad = (\max\{|\mathbf{C}_a + \alpha\mathbf{C}_b + \alpha^2\mathbf{C}_c| - r_a - r_b - r_c, 0\})^2. \end{aligned}$$

Hence, (27) is equivalent to

$$\begin{aligned} &(|\mathbf{C}_a + \alpha^2\mathbf{C}_b + \alpha\mathbf{C}_c| + r_a + r_b + r_c)^2 \\ &\le \epsilon^2(\max\{|\mathbf{C}_a + \alpha\mathbf{C}_b + \alpha^2\mathbf{C}_c| - r_a - r_b - r_c, 0\})^2 \end{aligned} \tag{28}$$

and (26b) can be handled similarly. In addition to the approximation by bound, we give other approximation techniques by further transforming (26) into the real domain using V_{abc}:

$$\left\{ \max_{V_{abc}\in\mathcal{V}_{in}} V_{abc}^\top(A_n - \epsilon^2 A_p)V_{abc} \right\} \le 0, \tag{29a}$$

$$\left\{\max_{V_{abc}\in\mathcal{V}_{in}} V_{abc}^{\top}(A_0-\epsilon^2 A_p)V_{abc}\right\}\le 0. \tag{29b}$$

where $V_{abc}^{\top}A_nV_{abc}=9\mathbf{V}_n\bar{\mathbf{V}}_n$, $V_{abc}^{\top}A_0V_{abc}=9\mathbf{V}_0\bar{\mathbf{V}}_0$, and $V_{abc}^{\top}A_pV_{abc}=9\mathbf{V}_p\bar{\mathbf{V}}_p$. Matrices $A_n\in\mathbb{R}^{6\times6}$, $A_p\in\mathbb{R}^{6\times6}$, and $A_0\in\mathbb{R}^{6\times6}$ can be calculated from (24) and have the following structure with off-diagonal matrices $B_n\in\mathbb{R}^{2\times2}$, $B_0\in\mathbb{R}^{2\times2}$, and $B_p\in\mathbb{R}^{2\times2}$

$$A_n=\begin{bmatrix}\mathbb{I}_2 & B_n & B_n^{\top}\\ B_n^{\top} & \mathbb{I}_2 & B_n\\ B_n & B_n^{\top} & \mathbb{I}_2\end{bmatrix},\ B_n=\begin{bmatrix}\cos(240^\circ) & -\sin(240^\circ)\\ \sin(240^\circ) & \cos(240^\circ)\end{bmatrix}, \tag{30a}$$

$$A_0=\begin{bmatrix}\mathbb{I}_2 & B_0 & B_0^{\top}\\ B_0^{\top} & \mathbb{I}_2 & B_0\\ B_0 & B_0^{\top} & \mathbb{I}_2\end{bmatrix},\ B_0=\begin{bmatrix}\cos(0^\circ) & -\sin(0^\circ)\\ \sin(0^\circ) & \cos(0^\circ)\end{bmatrix}, \tag{30b}$$

$$A_p=\begin{bmatrix}\mathbb{I}_2 & B_p & B_p^{\top}\\ B_p^{\top} & \mathbb{I}_2 & B_p\\ B_p & B_p^{\top} & \mathbb{I}_2\end{bmatrix},\ B_p=\begin{bmatrix}\cos(120^\circ) & -\sin(120^\circ)\\ \sin(120^\circ) & \cos(120^\circ)\end{bmatrix}. \tag{30c}$$

Both A_n and A_p are rank-two matrices and all four corresponding eigenvectors are orthogonal to each other. Hence, the matrix $A_n-\epsilon^2A_p$ is indefinite with rank four and the left-hand side (LHS) of (29a) is a nonconvex quadratically constrained quadratic program (QCQP) with multiple constraints. A similar conclusion holds for the LHS of (29b). General non-convex QCQPs are NP-hard to solve.

To effectively approximate the QCQP or its solution, we first give the following lemma that provides a necessary condition on the location of the optimal solutions. For the rest of the paper, we use (29a) and VUF_n as an example since (29b) and VUF_0 can be similarly handled with exactly the same theoretical properties.

Lemma 4.1. *If $V_{abc}^*=(V_a^*,V_b^*,V_c^*)^{\top}$ is optimal for (29a), then*

$$V_a^*\in\partial\mathcal{V}_{in}^a,\ V_b^*\in\partial\mathcal{V}_{in}^b,\ V_c^*\in\partial\mathcal{V}_{in}^c.$$

Proof. We prove by contradiction. First, we assume that $V_a^*\notin\partial\mathcal{V}_{in}^a$ and define a corresponding vector $\Delta_V=\hat{\alpha}u_V\in\mathbb{R}^6$ with scalar $\hat{\alpha}$ and $u_V=(1,0,0,0,0,0)^{\top}$. Then, we conclude that there exists $\delta>0$ such that $(V_{abc}^*+\Delta_V)\in\mathcal{V}_{in}$ for all $\{\hat{\alpha}\in\mathbb{R}:\ |\hat{\alpha}|<\delta\}$ since $V_a^*\notin\partial\mathcal{V}_{in}^a$. Next, we compare the optimal objective with the objective under $(V_{abc}^*+\Delta_V)$:

$$\begin{aligned}&(V_{abc}^*+\Delta_V)^{\top}(A_n-\epsilon^2A_p)(V_{abc}^*+\Delta_V)\\ &\qquad-(V_{abc}^*)^{\top}(A_n-\epsilon^2A_p)V_{abc}^*\\ =\ &\hat{\alpha}^2(u_V^{\top}(A_n-\epsilon^2A_p)u_V)+\hat{\alpha}(2u_V^{\top}(A_n-\epsilon^2A_p)V_{abc}^*)\\ =\ &\hat{\alpha}^2(1-\epsilon^2)+\hat{\alpha}(2u_V^{\top}(A_n-\epsilon^2A_p)V_{abc}^*)=f(\hat{\alpha}).\end{aligned} \tag{31}$$

Since $\epsilon<1$, we have $1-\epsilon^2>0$ and $f(\hat{\alpha})$ is a convex quadratic function of $\hat{\alpha}$. When $\hat{\alpha}=0$, we have $f(0)=0$ and hence we must also have $\max\{f(\frac{\delta}{2}),f(-\frac{\delta}{2})\}>0$. In other words, we can improve the optimal value of (29a) by choosing either $\hat{\alpha}=\frac{\delta}{2}$ or $-\frac{\delta}{2}$ and constructing a new solution $(V_{abc}^*+\Delta_V)\in\mathcal{V}_{in}$. Hence, this is contradictory with V_{abc}^* being optimal. Similar discussions apply to cases when $V_b^*\notin\partial\mathcal{V}_{in}^b$ and $V_c^*\notin\partial\mathcal{V}_{in}^c$ and the proof is complete. □

Using Lemma 4.1, we know that the optimal solution to (29a) falls on $\partial\mathcal{V}_{in}^a\times\partial\mathcal{V}_{in}^b\times\partial\mathcal{V}_{in}^c$ and hence the inequality constraint in (29a) is equivalent to

$$\left\{\max_{V_{abc}\in\partial\mathcal{V}_{in}^a\times\partial\mathcal{V}_{in}^b\times\partial\mathcal{V}_{in}^c} V_{abc}^{\top}(A_n-\epsilon^2A_p)V_{abc}\right\}\le 0, \tag{32}$$

since both maximizations in (29a) and (32) return the same optimal value. Next, we develop two approaches to approximate (32) or its solution.

4.3.1. Polytope approximation

First, we model three polytopes $\mathcal{P}^a\in\mathbb{R}^2$, $\mathcal{P}^b\in\mathbb{R}^2$, and $\mathcal{P}^c\in\mathbb{R}^2$ such that

$$\mathcal{V}_{in}^a\subset\mathcal{P}^a,\ \mathcal{V}_{in}^b\subset\mathcal{P}^b,\ \mathcal{V}_{in}^c\subset\mathcal{P}^c. \tag{33}$$

Denote the finite set of the extreme points of $\mathcal{P}^a$, $\mathcal{P}^b$, and $\mathcal{P}^c$ as $\mathcal{E}^a$, $\mathcal{E}^b$, and $\mathcal{E}^c$, respectively. We next present a theorem that provides a necessary condition on the location of the optimal solution for the maximization problem in

$$\left\{\max_{V_{abc}\in\mathcal{P}^a\times\mathcal{P}^b\times\mathcal{P}^c} V_{abc}^{\top}(A_n-\epsilon^2A_p)V_{abc}\right\}\le 0. \tag{34}$$

It is easy to see that (34) is a safe approximation of (29a) and (32) with a larger optimal value.

Theorem 4.1. *If $V_{abc}^*=(V_a^*,V_b^*,V_c^*)^{\top}$ is optimal for the maximization problem in (34), then*

$$V_a^*\in\mathcal{E}^a,\ V_b^*\in\mathcal{E}^b,\ V_c^*\in\mathcal{E}^c. \tag{35}$$

Proof. First, we claim that

$$V_a^*\in\partial\mathcal{P}^a,\ V_b^*\in\partial\mathcal{P}^b,\ V_c^*\in\partial\mathcal{P}^c \tag{36}$$

whose proof is similar to the one of Lemma 4.1.

Next, we show the theorem by contradiction. Since $V_a^*\in\partial\mathcal{P}^a$, then $V_a^*\in H^a$ where H^a is one of the hyperplanes defining $\partial\mathcal{P}^a$. Define H^a as $\{x\in\mathbb{R}^2:\ h^{\top}x=\tilde{h}\}$, then $h^{\top}V_a^*=\tilde{h}$. If we assume $V_a^*\notin\mathcal{E}^a$, then there exists $\delta>0$ and a direction $\{g\in\mathbb{R}^2:\ \|g\|=1,\ g^{\top}h=0\}$ such that $(V_a^*+\hat{\alpha}g)\in\partial\mathcal{P}^a$ for all $\{\hat{\alpha}\in\mathbb{R}:\ |\hat{\alpha}|<\delta\}$. Next, we compare the optimal objective with the objective under $(V_{abc}^*+\Delta_V)$ where $\Delta_V=\hat{\alpha}u_V\in\mathbb{R}^6$, $u_V=(g^{\top},0,0,0,0)^{\top}$, and get

$$\begin{aligned}&(V_{abc}^*+\Delta_V)^{\top}(A_n-\epsilon^2A_p)(V_{abc}^*+\Delta_V)\\ &\qquad-(V_{abc}^*)^{\top}(A_n-\epsilon^2A_p)V_{abc}^*\\ =\ &\hat{\alpha}^2(u_V^{\top}(A_n-\epsilon^2A_p)u_V)+\hat{\alpha}(2u_V^{\top}(A_n-\epsilon^2A_p)V_{abc}^*)\\ =\ &\hat{\alpha}^2(1-\epsilon^2)g^{\top}\mathbb{I}_2g+\hat{\alpha}(2u_V^{\top}(A_n-\epsilon^2A_p)V_{abc}^*)\\ =\ &\hat{\alpha}^2(1-\epsilon^2)+\hat{\alpha}(2u_V^{\top}(A_n-\epsilon^2A_p)V_{abc}^*)=f(\hat{\alpha}),\end{aligned} \tag{37}$$

which is a convex quadratic function on $\hat{\alpha}$ with $f(0)=0$ since $\epsilon<1$. Then, similar to Lemma 4.1, we conclude that we can improve the optimal value of (34) by using a new feasible solution $(V_{abc}^*+\Delta_V)$ with $\hat{\alpha}=\frac{\delta}{2}$ or $-\frac{\delta}{2}$. This contradicts the optimality of V_{abc}^*. Similar discussions are applicable to cases when $V_b^*\notin\mathcal{E}^b$ and $V_c^*\notin\mathcal{E}^c$ and the proof is complete. □

Now, we equivalently reformulate (34) as

$$\left\{\max_{V_{abc}\in\mathcal{E}^a\times\mathcal{E}^b\times\mathcal{E}^c} V_{abc}^{\top}(A_n-\epsilon^2A_p)V_{abc}\right\}\le 0 \tag{38}$$

and solving an optimization problem (34) becomes an evaluation problem on the set of extreme points.

There are many ways to find $\mathcal{P}^a$, $\mathcal{P}^b$, and $\mathcal{P}^c$. Here, we use a special polytope to analyze the optimality gap of the approximation. Since each polytope is in dimension 2, we propose to use the circumscribed regular polygon of the disk (CRP). For a unit closed disk $\bar{D}(1)$, the extreme points of a CRP with $2m$ ($m\ge2$) sides are as follows

$$\left\{\frac{1}{\cos(\frac{\pi}{2m})}\begin{bmatrix}\cos(\phi)\\ \sin(\phi)\end{bmatrix}:\ \phi=\frac{(2k-1)\pi}{2m},\ k=1,2,...,2m\right\}.$$

Note that while a CRP can have a phase shift, we do not consider this here for the sake of simplicity. In combination with C_{abc} and r_{abc}, we can easily find $\mathcal{E}^{a,2m}$, $\mathcal{E}^{b,2m}$, and $\mathcal{E}^{c,2m}$. We add $2m$ in the notations to denote the dimension of the CRP. By defining a general function $E^{2m}:\mathbb{R}^2\times\mathbb{R}\to\mathbb{R}^{2m}$, then $\mathcal{E}^a=E^{2m}(C_a,r_a)$ can be represented as

$$\left\{C_a + \frac{r_a}{\cos(\frac{\pi}{2m})}\begin{bmatrix}\cos(\phi)\\ \sin(\phi)\end{bmatrix}: \phi = \frac{(2k-1)\pi}{2m},\ k_a = 1, 2, ..., 2m\right\}.$$

We next show how the optimality gap between (32) and (38) is affected by the dimension m.

Corollary 4.1. *Denoting the optimal values of (32) and (38) as F_b^* and F_e^*, respectively, we have*

$$|F_e^* - F_b^*| \le |F_e^* - F_i^*|, \tag{39}$$

where F_i^* is the optimal solution of the following problem

$$\max_{V_{abc}\in\hat{\mathcal{E}}^a\times\hat{\mathcal{E}}^b\times\hat{\mathcal{E}}^c} V_{abc}^\top(A_n - \epsilon^2 A_p)V_{abc}, \tag{40}$$

in which

$$\hat{\mathcal{E}}^a = E^{2m}(C_a, r_a\cos(\frac{\pi}{2m})),$$
$$\hat{\mathcal{E}}^b = E^{2m}(C_b, r_b\cos(\frac{\pi}{2m})),$$
$$\hat{\mathcal{E}}^c = E^{2m}(C_c, r_c\cos(\frac{\pi}{2m})).$$

We also have

$$\lim_{m\to+\infty} |F_e^* - F_i^*| = 0. \tag{41}$$

Proof. We prove (39) by demonstrating the relationship

$$F_e^* \ge F_b^* \ge F_i^*.$$

The first inequality results from the fact that (38) is a safe approximation of (32). The second inequality is true because $\hat{\mathcal{E}}^a \subset \partial\mathcal{V}_{in}^a$ (same for phases b and c). Hence, (32) is more conservative than (40).

Next, we prove (41). Given any $m \ge 2$, we have the following inequality

$$|F_e^* - F_i^*| \le \max_{k_a\in\mathcal{K},k_b\in\mathcal{K},k_c\in\mathcal{K}} |J(V_{abc}^e) - J(V_{abc}^i)|, \tag{42}$$

where $J(V_{abc}) = V_{abc}^\top(A_n - \epsilon^2 A_p)V_{abc}$. V_{abc}^e and V_{abc}^i are a corresponding pair in $\mathcal{E}^a\times\mathcal{E}^b\times\mathcal{E}^c$ and $\hat{\mathcal{E}}^a\times\hat{\mathcal{E}}^b\times\hat{\mathcal{E}}^c$ with the same k_a, k_b, and k_c. $\mathcal{K}$ denotes the integer set on $[1, 2m]$. We show that (42) is valid by substituting a special $(k_a, k_b, k_c)^\top$ that is optimal for (38) into the right-hand side of (42). The inequality holds with the special choice of $(k_a, k_b, k_c)^\top$ and hence (42) is true. Further, we have

$$\|V_{abc}^e - V_{abc}^i\| = \left(\frac{1}{\cos(\frac{\pi}{2m})} - 1\right)\|r_{abc}\|,\ \ \forall\ (k_a, k_b, k_c)^\top \in \mathcal{K}^3 \tag{43}$$

since V_{abc}^e and V_{abc}^i are a corresponding pair. Meanwhile, $J(V_{abc})$ is continuously differentiable and hence Lipschitz on compact set $\bar{D}(C_a, \sqrt{2}r_a)\times\bar{D}(C_b, \sqrt{2}r_b)\times\bar{D}(C_c, \sqrt{2}r_c)$. We choose this compact set since it contains all the feasible sets of (38) and (40) for all $m \ge 2$. Denote the Lipschitz constant as L. For all $m \ge 2$, we have

$$\max_{k_a\in\mathcal{K},k_b\in\mathcal{K},k_c\in\mathcal{K}} |J(V_{abc}^e) - J(V_{abc}^i)| \le \max_{k_a\in\mathcal{K},k_b\in\mathcal{K},k_c\in\mathcal{K}} L\|V_{abc}^e - V_{abc}^i\|. \tag{44}$$

Combining (42), (43), and (44), we have

$$\lim_{m\to+\infty} |F_e^* - F_i^*| \le \lim_{m\to+\infty}\max_{k_a\in\mathcal{K},k_b\in\mathcal{K},k_c\in\mathcal{K}} L\|V_{abc}^e - V_{abc}^i\|$$
$$= \lim_{m\to+\infty}\left(\frac{1}{\cos(\frac{\pi}{2m})} - 1\right)L\|r_{abc}\| = 0.$$

The last equality holds since $\lim_{m\to+\infty}\cos(\frac{\pi}{2m}) = 1$. Further, since $|F_e^* - F_i^*|$ is non-negative, based on squeeze theorem, the proof is complete. □

This result tells us that as we increase m (i.e., the number of sides of the CRP), the safe approximation (38) asymptotically converges to the true optimal value of (29a) or (32).

4.3.2. Semidefinite and Lagrangian relaxation

Other conventional techniques [22,23] for general QCQP problems use semidefinite relaxation (SDR) or Lagrangian relaxation (LGR). The SDR of (32) (shown below) is derived by lifting the vector space of the variable V_{abc} to the matrix space $W_{abc} \in \mathbb{R}^{6\times6}$ and relaxing the rank-one constraints from $W_{abc} = V_{abc}V_{abc}^\top$ to get a convex constraint $W_{abc} \succeq V_{abc}V_{abc}^\top$ and the following semidefinite programming (SDP) problem. Since the original problem in (32) is maximization, both LGR and SDR give higher optimal values and hence a safe approximation to (32):

$$\begin{aligned}(\text{SDR})\ \max\quad & \mathrm{Tr}((A_n - \epsilon^2 A_p)W_{abc})\\ \text{s.t.}\quad & W_{abc,11} + W_{abc,22} - 2C_a^\top V_a + \|C_a\|^2 = r_a^2,\\ & W_{abc,33} + W_{abc,44} - 2C_b^\top V_b + \|C_b\|^2 = r_b^2,\\ & W_{abc,55} + W_{abc,66} - 2C_c^\top V_c + \|C_c\|^2 = r_c^2,\\ & W_{abc} \succeq V_{abc}V_{abc}^\top\end{aligned}$$

LGR uses Lagrangian duality to derive an SDP-based reformulation as follows

$$\begin{aligned}(\text{LGR})\ \min_{\mu\in\mathbb{R}^3}\quad & \gamma\\ \text{s.t.}\quad & Y = \begin{bmatrix}Q(\mu) & q(\mu)\\ q(\mu)^\top & r(\mu)\end{bmatrix},\\ & Y \succeq 0\end{aligned}$$

where

$$Q(\mu) = -(A_n - \epsilon^2 A_p + \mathrm{blkdiag}(\mu_1\mathbb{I}_2, \mu_2\mathbb{I}_2, \mu_3\mathbb{I}_2)),$$
$$q(\mu) = (-\mu_1 C_a^\top, -\mu_2 C_b^\top, -\mu_3 C_c^\top)^\top,$$
$$r(\mu) = \gamma - \mu_1(\|C_a\|^2 - r_a^2) - \mu_2(\|C_b\|^2 - r_b^2) - \mu_3(\|C_c\|^2 - r_c^2).$$

Then, (32) can be safely approximated as

$$\gamma \le 0,\ \ \mu \in \mathbb{R}^3,\ \ \begin{bmatrix}Q(\mu) & q(\mu)\\ q(\mu)^\top & r(\mu)\end{bmatrix} \succeq 0. \tag{45}$$

Existing work [23] shows that SDR and LGR are dual to each other. Strong duality also holds here as both SDR and LGR are strictly feasible (i.e., there exists positive definite matrix solutions).[4] Since (32) is nonconvex, there is a gap between SDR or LGR with the true optimal solutions. Next, we give conditions on C_{abc} and r_{abc} such that SDR and LGR have the same optimal value to (32). Duality gaps have also been analyzed for typical optimal power flow formulations in, e.g., [24–27]. In this paper, we focus on different type of constraint related to voltage balance requirements.

We start from LGR and show a sufficient condition such that strong duality holds between LGR and (32). The conditions can also be efficiently evaluated by solving three small convex QCQPs. For concise derivation, we define three sets:

$$\bar{D}_{abc} = \bar{D}(r_a)\times\bar{D}(r_b)\times\bar{D}(r_c),$$
$$D_{abc} = D(r_a)\times D(r_b)\times D(r_c),$$
$$\partial\bar{D}_{abc} = \partial\bar{D}(r_a)\times\partial\bar{D}(r_b)\times\partial\bar{D}(r_c).$$

Theorem 4.2. *If conditions*

[4] In SDR, we can select $V_{abc} = 0$ and pick W_{abc} to be diagonal with strictly positive elements. In LGR, we can choose any $\mu < -\lambda_{\max}(A_n - \epsilon^2 A_p)$, then $Q(\mu)$ is positive definite. Then, based on the Schur complement, we can always choose γ large enough that $r(\mu) - q(\mu)^\top P(\mu)^{-1}q(\mu) > 0$.

$$f_{i,i+1} \notin [-r_i, r_i] \times [-r_{i+1}, r_{i+1}], \quad i = 1, 3, 5, \tag{46a}$$

$$\left\{ \min_{Y_a \in \bar{D}_{abc}} \|(2BY_a + f)_{1,2}\|^2 \right\} \geq 4(2+\epsilon^2)^2 r_a^2, \tag{46b}$$

$$\left\{ \min_{Y_b \in \bar{D}_{abc}} \|(2BY_b + f)_{3,4}\|^2 \right\} \geq 4(2+\epsilon^2)^2 r_b^2, \tag{46c}$$

$$\left\{ \min_{Y_c \in \bar{D}_{abc}} \|(2BY_c + f)_{5,6}\|^2 \right\} \geq 4(2+\epsilon^2)^2 r_c^2, \tag{46d}$$

where

$$B = (\epsilon^2 A_p - A_n) - \lambda_{\min}(\epsilon^2 A_p - A_n)\mathbb{I}_6,$$
$$f = 2(\epsilon^2 A_p - A_n) C_{abc},$$
$$r_i = 2(r_a \|B_i^{1,2}\| + r_b \|B_i^{3,4}\| + r_c \|B_i^{5,6}\|), \quad i = 1, .., 6,$$

are satisfied by certain C_{abc} and r_{abc}, then strong duality holds between LGR and (32).

Proof. We prove strong duality for the following problem:

$$\min_{V_{abc} \in \partial\mathcal{V}_{in}^a \times \partial\mathcal{V}_{in}^b \times \partial\mathcal{V}_{in}^c} V_{abc}^\top (\epsilon^2 A_p - A_n) V_{abc}. \tag{47}$$

If strong duality holds for (47), strong duality also holds for (32) since their duals always have opposite optimal values. Define $Y_{abc} = (Y_a, Y_b, Y_c)^\top = V_{abc} - C_{abc}$ and $A = \epsilon^2 A_p - A_n$. We rewrite (47) as

$$\min_{Y_{abc} \in \partial \bar{D}_{abc}} (Y_{abc} + C_{abc})^\top A (Y_{abc} + C_{abc}),$$

where

$$(Y_{abc} + C_{abc})^\top A (Y_{abc} + C_{abc}) = Y_{abc}^\top (A - \lambda \mathbb{I}_6) Y_{abc} + 2C_{abc}^\top A Y_{abc} + C_{abc}^\top A C_{abc} + \lambda Y_{abc}^\top Y_{abc}.$$

Since $Y_{abc} \in \partial\bar{D}_{abc}$, we ignore the last two terms (constant-valued) and pick $\lambda = \lambda_{\min}(A) = -3$ such that $B = (A - \lambda\mathbb{I}_6) \succeq 0$. Define $f = 2AC_{abc}$. We then obtain

$$\min_{Y_{abc} \in \partial \bar{D}_{abc}} Y_{abc}^\top B\, Y_{abc} + f^\top Y_{abc}. \tag{48}$$

A sufficient condition ensuring that strong duality holds for (48) is when the following problem

$$\min_{Y_{abc} \in \bar{D}_{abc}} Y_{abc}^\top B\, Y_{abc} + f^\top Y_{abc} \tag{49}$$

has its optimal solution on $\partial\bar{D}_{abc}$ under certain requirements on C_{abc} and r_{abc}. We leave the proof of this to the following lemma. Now, we assume $Y^* = (Y_a^*, Y_b^*, Y_c^*)^\top$ to be any point in $\bar{D}_{abc}$ and $Y_a^* \notin \partial\bar{D}(r_a)$ without loss of generality since similar discussions can apply to Y_b^* and Y_c^*. The sufficient condition for strong duality is satisfied if there exists a direction $\{g_a \in \mathbb{R}^2 : \|g_a\| = 1\}$ in the space of Y_a such that the objective can be improved when Y_a^* moves to $\partial\bar{D}(r_a)$. Denote $\Delta_Y = d(g_a, 0, 0, 0, 0)^\top$ where $d \geq 0$ denotes the distance moving along the direction Δ_Y. We compare the objective at $Y^* + \Delta_Y$ and Y^* and get

$$\begin{aligned} &(Y^* + \Delta_Y)^\top B (Y^* + \Delta_Y) + f^\top (Y^* + \Delta_Y) \\ &\qquad - (Y^*)^\top B\, Y^* - f^\top Y^* \\ =\ & d^2(2+\epsilon^2) + d\, h_a^\top g_a = f(d, g_a) \end{aligned} \tag{50}$$

where $h_a = (2BY^* + f)_{1,2}$. We cannot have $h_a = 0$ since there does not exist a direction g_a that improves the objective. Denote $(2BY^*)_i = 2B_i^\top Y^* = 2B_i^{1,2} Y_a^* + 2B_i^{3,4} Y_b^* + 2B_i^{5,6} Y_c^*$. Since Y^* is in a compact set $\bar{D}_{abc}$, we can find the tight bound $|(2BY^*)_i| \leq r_i = 2(r_a \|B_i^{1,2}\| + r_b \|B_i^{3,4}\| + r_c \|B_i^{5,6}\|)$. Further, if $f_{1,2} \notin [-r_1, r_1] \times [-r_2, r_2]$, then $h_a \neq 0$ for all possible $Y^* \in \bar{D}_{abc}$.

Next, since $f(d, g_a)$ is a convex quadratic function of d with fixed second-order coefficient, we know the steepest descent direction is $-h_a/\|h_a\|$ (i.e., for any fixed d, $g_a = -h_a/\|h_a\|$ minimizes $f(d, g_a)$). Hence, we fix $g_a = -h_a/\|h_a\|$ without loss of optimality. The objective is improved if $f(d, -h_a/\|h_a\|) \leq 0$, which is equivalent to $d \in [0, \frac{\|h_a\|}{2+\epsilon^2}]$. Hence, if we require $\frac{\|h_a\|}{2+\epsilon^2} \geq 2r_a$, then there must exists a point on $\partial\bar{D}(r_a)$ with certain $d^* \in (0, \frac{\|h_a\|}{2+\epsilon^2})$ that improves the objective. Since Y^* can be any point in $\bar{D}_{abc}$, our requirement becomes

$$\begin{aligned} &\left\{ \min_{Y^* \in \bar{D}_{abc}} \|h_a\| \right\} \geq 2(2+\epsilon^2) r_a \\ \Leftrightarrow\ &\left\{ \min_{Y^* \in \bar{D}_{abc}} h_a^\top h_a \right\} \geq 4(2+\epsilon^2)^2 r_a^2. \end{aligned} \tag{51}$$

The left-hand side of (51) is a convex QCQP[5] and hence can be solved easily. Similar analyses for phases b and c complete the proof. □

Lemma 4.2. *For given C_{abc} and r_{abc}, if (49) has its optimal solution on $\partial\bar{D}_{abc}$, then (48) has strong duality.*

Proof. For simplicity, generalize (48) as

$$\min f(x) \text{ s.t. } g_i(x) = 0, \quad i = 1, \ldots, m,$$

which is equivalent to

$$v_1^* = \{\min f(x) \text{ s.t. } g_i(x) \geq 0, \ g_i(x) \leq 0, \ i = 1, \ldots, m\}$$

with optimal value v_1^*. The associated Lagrangian dual is

$$h_1^* = \max_{\lambda \geq 0, \mu \geq 0} \inf_x f(x) + \Sigma_i^m \lambda_i g_i(x) - \Sigma_i^m \mu_i g_i(x) \tag{52}$$

with optimal value h_1^*. Similarly, (49) can be represented as

$$v_2^* = \{\min f(x) \text{ s.t. } g_i(x) \leq 0, \ i = 1, \ldots, m\}$$

with the following Lagrangian dual problem

$$h_2^* = \max_{\lambda \geq 0} \inf_x f(x) + \Sigma_i^m \lambda_i g_i(x) \tag{53}$$

and has optimal values v_2^* (h_2^* for (53)).

Denote the optimal solution to (53) as x^* and λ^*. Observe that (53) is a special case of (52) with $\mu = 0$. Hence, we have $h_1^* \geq h_2^*$. Since (49) is a convex QCQP with nonempty interior, we also have strong duality such that $v_2^* = h_2^*$. Meanwhile, we also have $v_1^* = v_2^*$ (since (49) has its optimal solution on $\partial\bar{D}_{abc}$) and $h_1^* \leq v_1^*$ (weak duality). We conclude $h_1^* = v_1^*$ and hence strong duality holds for (48). □

Theorem 4.2 implies that when C_{abc} has relatively larger magnitudes than r_{abc}, there is a higher chance of having strong duality between LGR and (32). Next, we start with SDR and show that under certain conditions, even if r_{abc} has large magnitudes, we have exactness (i.e., the same optimal values) between SDR and (32). First, we give a general result for a QCQP problem whose SDR is exact.

Theorem 4.3. *Consider the following QCQP problem on $x_{abc} = (x_a, x_b, x_c)^\top \in \mathbb{R}^6$:*

$$\max_{x_{abc} \in \partial\bar{D}_{abc}} x_{abc}^\top A x_{abc} \tag{54}$$

where A has the following structure

$$A = \begin{bmatrix} \lambda\mathbb{I}_2 & B & B^\top \\ B^\top & \lambda\mathbb{I}_2 & B \\ B & B^\top & \lambda\mathbb{I}_2 \end{bmatrix}, \quad B = \begin{bmatrix} b_1 & -b_2 \\ b_2 & b_1 \end{bmatrix}.$$

Then, the following SDP relaxation is exact for (54):

[5] Strong duality holds since Slater's condition is satisfied (i.e., pick $Y^* \in D_{abc}$). Hence, (51) can also be equivalently transformed into SDP constraints.

$$\begin{aligned} \max \quad & \mathrm{Tr}(AX_{abc}) \\ \text{s.t.} \quad & X_{abc,11} + X_{abc,22} = r_a^2, \\ & X_{abc,33} + X_{abc,44} = r_b^2, \\ & X_{abc,55} + X_{abc,66} = r_c^2, \\ & X_{abc} \succeq 0. \end{aligned} \tag{55}$$

Proof. We prove the exactness by rewriting (54) into a homogeneous complex QCQP with the transformation $\mathbf{x}_{abc} = (x_{a,1} + \boldsymbol{j}x_{a,2}, x_{b,1} + \boldsymbol{j}x_{b,2}, x_{c,1} + \boldsymbol{j}x_{c,2})^\top$:

$$\begin{aligned} (54) \Leftrightarrow \max \quad & \mathbf{x}_{abc}^{\mathrm{H}} \mathbf{A} \mathbf{x}_{abc} \\ \text{s.t.} \quad & \mathbf{x}_{abc}^{\mathrm{H}} [\mathrm{blkdiag}(1, \mathcal{O}_2)] \mathbf{x}_{abc} = r_a^2, \\ & \mathbf{x}_{abc}^{\mathrm{H}} [\mathrm{blkdiag}(0, 1, 0)] \mathbf{x}_{abc} = r_b^2, \\ & \mathbf{x}_{abc}^{\mathrm{H}} [\mathrm{blkdiag}(\mathcal{O}_2, 1)] \mathbf{x}_{abc} = r_c^2, \end{aligned} \tag{56}$$

where

$$\mathbf{A} = \begin{bmatrix} \lambda & b_1 + \boldsymbol{j}b_2 & b_1 - \boldsymbol{j}b_2 \\ b_1 - \boldsymbol{j}b_2 & \lambda & b_1 + \boldsymbol{j}b_2 \\ b_1 + \boldsymbol{j}b_2 & b_1 - \boldsymbol{j}b_2 & \lambda \end{bmatrix}.$$

Then, based on Theorem 3.2 in [28,29], the SDP relaxation of (56) has a solution $\mathbf{X}_{abc} \in \mathcal{H}^3$ with $\mathrm{rank}(\mathbf{X}_{abc}) \le \lfloor \sqrt{l} \rfloor$ where l equals the number of equality constraints in (56) (i.e., $l = 3$). Hence, $\mathrm{rank}(\mathbf{X}_{abc}) \le 1$ and is thus exact for (56). Since (55) is a real-variable representation of the SDP relaxation of (56), the proof is complete.[6] □

To see how Theorem 4.3 is relevant to (32), we reformulate (32) by substituting $Y_{abc} = V_{abc} - C_{abc}$ and ignoring the constant to obtain

$$\max_{Y_{abc} \in \partial \tilde{D}_{abc}} Y_{abc}^\top (A_n - \epsilon^2 A_p) Y_{abc} + 2((A_n - \epsilon^2 A_p) C_{abc})^\top Y_{abc},$$

which satisfies Theorem 4.3 if $(A_n - \epsilon^2 A_p) C_{abc} = 0$. Since strong duality holds between LGR and SDR, Theorem 4.3 also guarantess strong duality between LGR and (32). Further, we see that Theorems 4.2 and 4.3 are not directly comparable (i.e., it is not the case that one is always stronger than the other). Theorem 4.2 can handle cases when C_{abc} has large magnitude relative to r_{abc}. However, Theorem 4.3 works when C_{abc} has a small magnitude compared to $A_n - \epsilon^2 A_p$ or belongs to $N(A_n - \epsilon^2 A_p)$ (approximately $N(A_n)$ when ϵ is small). Hence, each condition has its own advantages. In practice, Theorem 4.2 is more applicable as the condition is better aligned with the characteristics of practical distribution networks.

4.4. Balancibility condition

Using the closed-form reformulations or approximations of the voltage balance requirements from the three different unbalance definitions, we can now obtain the full balancibility condition by connecting the $\mathcal{V}_L$ from the solvability condition (8) to these voltage balance requirements. We briefly discussed this connection when we first introduced C_{abc} and r_{abc} in Section 4. Here, we give an example of the complete balancibility condition using the polytope approximation under the VUF_n definition. Without loss of generality, assume $i^* \in \mathcal{N}_L$ is the critical node with a voltage unbalance tolerance of ϵ and there is no degeneracy (i.e., $\min_{p \in \{a,b,c\}} \xi_{i^*,p}(\mathbf{S}_L) > 0$). Then, the full balancibility condition is:

$$(6) \text{ and } \left\{ \max_{V_{abc} \in \mathcal{E}^a \times \mathcal{E}^b \times \mathcal{E}^c} V_{abc}^\top (A_n - \epsilon^2 A_p) V_{abc} \right\} \le 0 \tag{57}$$

where

$$\mathcal{E}^p = E^{2m}((\mathrm{Re}(\mathbf{C}_p), \mathrm{Im}(\mathbf{C}_p))^\top, r_p),$$

$\mathbf{C}_p = (1 - \eta_{i^*,p}(\sigma_L))\, \mathbf{E}_p^{i^*} \mathbf{v}_{L,p}^{0,i^*}$, and $r_p = r|\mathbf{E}_p^{i^*} \mathbf{v}_{L,p}^{0,i^*}| \xi_{i^*,p}(\mathbf{S}_L)$ for all $p \in \{a, b, c\}$. Note that the solvability condition can be simultaneously combined with multiple voltage balance requirements. Particularly for *VUF* definitions, since C_{abc} and r_{abc} can be determined if $\mathbf{S}_L$ is provided, the sufficient conditions in Theorems 4.2 and 4.3 can be evaluated to give better guidance regarding whether we should choose a polytope approximation or LGR.

All of the constraints in the balancibility condition are functions of $\mathbf{S}_L$. Hence, the balancibility condition defines a secure region of $\mathbf{S}_L$ such that a unique and balanced power flow solution is guaranteed to exist. There are multiple applications of the balancibility condition, such as directly incorporating the condition in an optimization problem. This condition then provides a feasible set on $\mathbf{S}_L$ that can directly replace the power flow equations to obtain associated robust voltage balance guarantees for the power flow solutions under uncertainty. Another application uses the balancibility condition in an iterative/decentralized algorithm such that each step provides an instance of $\mathbf{S}_L$. In this case, the balancibility condition can be used as an effective evaluation tool on $\mathbf{S}_L$ to provides quick solution existence, uniqueness, and voltage balance guarantees without solving the full power flow problem.

5. Case study

This section first provides case studies to compare the approximations of the voltage balance requirement under the definition of VUF_n and then demonstrates the results of the balancibility conditions using *PVUR, LVUR*, and VUF_n.

5.1. Tightness of VUF approximations

Here, we present instances of C_{abc} and r_{abc} to compare the results using approximation by bound (27), polytope approximation (38), and LGR (45). To get an estimate of the true optimal value of (32), we randomly generate 5×10^5 points on $\partial \mathcal{V}_{in}^a \times \partial \mathcal{V}_{in}^b \times \partial \mathcal{V}_{in}^c$ and find the maximum value over the samples.[7] For polytope approximation, we use $m = 2, 4, 8, 16, 32$.

As the first test, we select a center $C_a = (2, 0)^\top$, $C_b = (-1, -\sqrt{3})^\top$, and $C_c = (-1, \sqrt{3})^\top$ (a balanced center for phases *a, b, c*); radius $r_a = r_b = r_c = 0.6$; and tolerance $\epsilon = 0.3$. Fig. 2 shows optimality gaps (i.e., the absolute difference from the estimate using sampling method) of the approximation by bound, LGR, and polytope approximations using different m. When m is small, the polytope approximation has large optimality gap but the gap rapidly converges to zero as m increases. LGR does not have strong duality (i.e., non-zero optimality gap) and hence gradually loses its advantage to the polytope approximation when m increases. Approximation by bound provides an upper bound for the other approximation techniques.

As the second test, we select center $C_a = (3, 0)^\top$, $C_b = (-1, -\sqrt{3})^\top$, and $C_c = (-1, \sqrt{3})^\top$; radius $r_a = r_b = r_c = 0.1$; and tolerance $\epsilon = 0.1$, which satisfy the sufficient conditions in Theorem 4.2. We then show the same groups of optimality gaps in Fig. 3. Since strong duality holds between LGR and (32), we clearly see zero optimality gap in LGR. Meanwhile, the polytope approximation gradually converges to zero optimality gap as m increases and the approximation by bound gives an upper bound.

In practice, the tolerance ϵ is small ($\lesssim 5\%$). Thus, when the set $\mathbf{U}_{in}$ (or, equivalently, $\mathcal{V}_{in}$) is small (i.e., the radius r_{abc} is small), LGR has a higher chance of having a smaller optimality gap compared to the polytope approximation since Theorem 4.2 is easier to satisfy.

[6] Note that exactness is not guaranteed for any other QCQP formulations (e.g., (32)) that are either non-homogeneous or involve more than three equality constraints in complex-variable representation.

[7] The sampling method is unsecure to directly use in the balancibility condition since it is a relaxation to (32) and hence underestimates the voltage unbalance level.

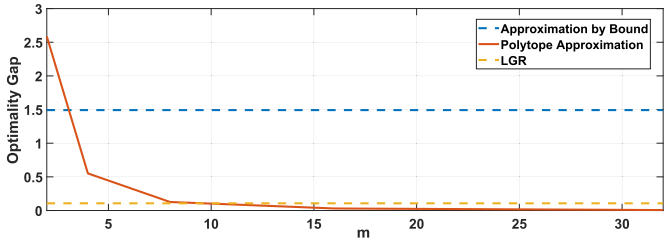

Fig. 2. Optimality Gaps of Approximation by Bound, Polytope Approximation, and LGR without Strong Duality.

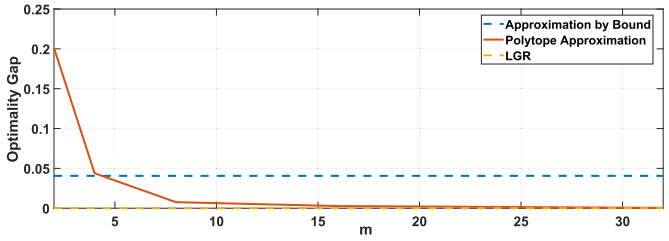

Fig. 3. Optimality Gaps of Approximation by Bound, Polytope Approximation, and LGR with Strong Duality.

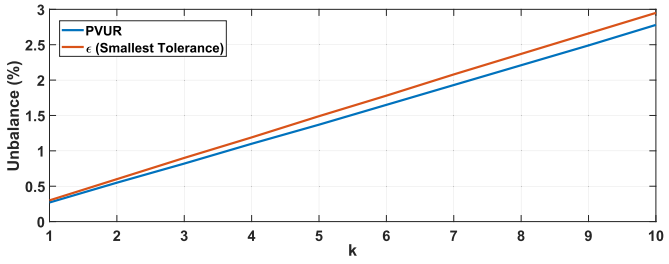

Fig. 4. Smallest Tolerance ϵ vs. "True" PVUR under $\mathbf{S}_L$ for different k.

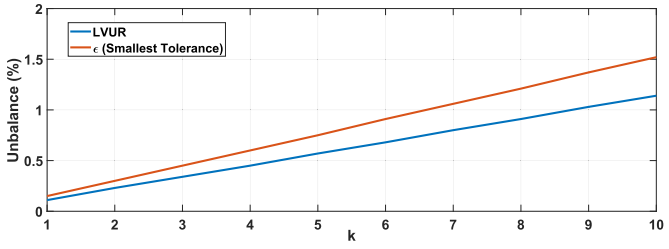

Fig. 5. Smallest Tolerance ϵ vs. "True" LVUR under $\mathbf{S}_L$ for different k.

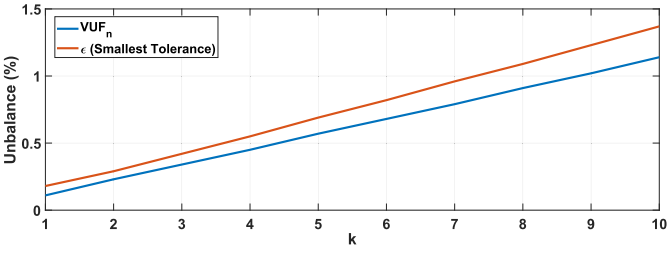

Fig. 6. Smallest Tolerance ϵ vs. "True" VUF under $\mathbf{S}_L$ for different k.

5.2. Balancibility conditions

To test the balancibility condition, we use a five-bus example system adopted from [30] by only considering wye-connected PQ loads. As the nominal point $\mathbf{S}_L^0$, we choose a group of balanced loads on bus 4 (10 kW) and bus 5 (50 kW) and consider unbalanced loading at bus 5 via $\boldsymbol{\sigma}_L$ (i.e., incremental loads $\mathbf{S}_L - \mathbf{S}_L^0$). For *LVUR* and *VUF*$_n$, we use the method of line-to-line voltage bounds (21) and LGR (45) respectively. For the set up, we select $\boldsymbol{\sigma}_L^5 = (10k, -5k, -5k)$ kW with $k = 1, 2, \ldots, 10$ and choose bus 4 as the critical node with respect to voltage balance.

To compare the quality of the balancibility condition, we first seek the smallest tolerance ϵ such that the voltage balance requirements are satisfied over the $\mathcal{V}_L$ that results from the solvability condition (6). Then, we find the true unbalance by solving the power flow equations with $\mathbf{S}_L$ and plugging the results into the unbalance definitions.

Figs. 4, 5, and 6 show the true unbalance level and the smallest tolerance level ϵ under different unbalance definitions. As k increases, the load at bus 5 becomes more unbalanced and hence induces a larger voltage unbalance level. We also see that there is a gap between ϵ and the true voltage unbalance level. The gap results from the fact that the balancibility condition provides voltage balance guarantees over $\mathcal{V}_L$, which contains the true solution $\mathbf{V}_L$ and hence a safe approximation. Since the gap is small, we conclude that the balancibility condition closely characterizes the system unbalance levels with the information of $\mathcal{V}_L$ without relying on the exact power flow solution $\mathbf{V}_L$. As k increases, $\mathcal{V}_L$ gets larger and hence results in a larger absolute gap. However, the ratio between ϵ and true unbalance level is approximately decreasing, which indicates reduced conservativeness. Further, we note that this conservativeness is system-dependent and can be improved if the solvability conditions (or general sets $\mathbf{U}_{in}$) are tighter.

6. Conclusions and future work

In this paper, we have proposed a concept called a *balancibility condition* which combines the existing power flow solution tools (e.g., solvability conditions) with voltage balance requirements. The balancibility condition quantifies a power injection region which is guaranteed to have a unique and balanced power flow solution. We considered unbalance definitions from multiple organizations and derived closed-form reformulations or approximations to quantify the voltage unbalance level. We used a general model to describe the sets that contain the power flow solutions under uncertain power injections and gave theoretical guarantees on the quality of the approaches. We numerically compared these approaches and demonstrated the benefits from the theoretical guarantees. We also compared the balancibility conditions associated with different unbalance definitions and demonstrated that the balancibility condition closely reflects the voltage unbalance level without excessive conservativeness.

Relevant future work includes testing all of the balancibility conditions and approaches on more general and realistic distribution network models (e.g., systems with delta-connected loads and ZIP loads). Other future work includes improving the quality of the balancibility condition by optimizing the solvability condition together with the voltage balance requirements. Finally, we will consider relevant applications of the balancibility conditions, including robust ACOPF problems.

Declaration of Competing Interest

The authors declare that they have no known competing financial interests or personal relationships that could have appeared to influence the work reported in this paper.

References

[1] A. von Jouanne, B. Banerjee, Assessment of voltage unbalance, IEEE Trans. Power Delivery 16 (4) (2001) 782–790.
[2] C.-Y. Lee, Effects of unbalanced voltage on the operation performance of a three-phase induction motor, IEEE Trans. Energy Convers. 14 (2) (1999) 202–208.
[3] U.S. Department of Energy, Eliminate voltage unbalance, Energy Tips: Motor Systems, (2012).
[4] U.S. Department of Energy, Stopping a Costly Leak: The Effects of Unbalanced Voltage on the Life and Efficiency of Three-Phase Electric Motors, Energy Matters, 2005.

[5] EMC Part 2-2: Environment Compatibility Levels for Low Frequency Conducted Disturbances and Signalling in Public Low-Voltage Power Supply Systems, IEC 61000-2-2, (2002).
[6] IEEE Recommended Practice for Monitoring Electric Power Quality, IEEE Standard 1159, (2009).
[7] NEMA Standard for Motors and Generators, ANSI/NEMA Standard MG1, (1993).
[8] IEEE Recommended Practice for Electric Power Distribution for Industrial Plants, IEEE Standard 141, (1993).
[9] IEEE Guide for Self-Commutated Converters, IEEE Standard 936, (1987).
[10] T.-H. Chen, C.-H. Yang, N.-C. Yang, Examination of the definitions of voltage unbalance, Int. J. Electric. Power Energy Syst. 49 (2013) 380–385.
[11] K. Girigoudar, D.K. Molzahn, L.A. Roald, On the relationships among different voltage unbalance definitions, North American Power Symposium (NAPS), (2019). Wichita, KS
[12] D. Lee, H.D. Nguyen, K. Dvijotham, K. Turitsyn, Convex restriction of power flow feasibility sets, IEEE Trans. Control Network Syst. (3) (2019) 1235–1245.
[13] K. Dvijotham, H.D. Nguyen, K. Turitsyn, Solvability regions of affinely parameterized quadratic equations, IEEE Control Syst. Lett. 2 (1) (2018) 25–30.
[14] B. Cui, X.A. Sun, Solvability of power flow equations through existence and uniqueness of complex fixed point, arXiv:1904.08855(2019).
[15] S. Bolognani, S. Zampieri, On the existence and linear approximation of the power flow solution in power distribution networks, IEEE Trans. Power Syst. 31 (1) (2016) 163–172.
[16] C. Wang, A. Bernstein, J.-Y. Le Boudec, M. Paolone, Explicit conditions on existence and uniqueness of load-flow solutions in distribution networks, IEEE Trans. Smart Grid 9 (2) (2018) 953–962.
[17] C. Wang, A. Bernstein, J.-Y. Le Boudec, M. Paolone, Existence and uniqueness of load-flow solutions in three-phase distribution networks, IEEE Trans. Power Syst. 32 (4) (2017) 3319–3320.
[18] A. Bernstein, C. Wang, E. Dall'Anese, J.-Y. Le Boudec, C. Zhao, Load flow in multiphase distribution networks: existence, uniqueness, non-singularity and linear models, IEEE Trans. Power Syst. 33 (6) (2018) 5832–5843.
[19] H.D. Nguyen, K. Dvijotham, S. Yu, K. Turitsyn, A framework for robust long-term voltage stability of distribution systems, IEEE Trans. Smart Grid 10 (5) (2019) 4827–4837.
[20] K. Girigoudar, L.A. Roald, On the impact of different voltage unbalance metrics in distribution system optimization, Electric Power Systems Research (2020). to be presented at 21st Power Systems Computation Conference (PSCC)
[21] M. Bazrafshan, N. Gatsis, Convergence of the Z-bus method for three-phase distribution load-flow with ZIP loads, IEEE Trans. Power Syst. 33 (1) (2018) 153–165.
[22] S. Boyd, L. Vandenberghe, Convex Optimization, Cambridge University Press, 2004.
[23] J. Park, S. Boyd, General heuristics for nonconvex quadratically constrained quadratic programming, arXiv:1703.07870 (2017).
[24] J. Lavaei, S.H. Low, Zero duality gap in optimal power flow problem, IEEE Trans. Power Syst. 27 (1) (2012) 92–107.
[25] B.C. Lesieutre, D.K. Molzahn, A.R. Borden, C.L. DeMarco, Examining the Limits of the Application of Semidefinite Programming to Power Flow Problems, 49th Annual Allerton Conference on Communication, Control, and Computing (Allerton), (2011), pp. 1492–1499.
[26] C.W. Tan, D.W.H. Cai, X. Lou, Resistive network optimal power flow: uniqueness and algorithms, IEEE Trans. Power Syst. 30 (1) (2015) 263–273.
[27] D.K. Molzahn, B.C. Lesieutre, C.L. DeMarco, Investigation of non-zero duality gap solutions to a semidefinite relaxation of the optimal power flow problem, 47th Hawaii International Conference on System Sciences (HICSS), (2014).
[28] Y. Huang, D.P. Palomar, Rank-constrained separable semidefinite programming with applications to optimal beamforming, IEEE Trans. Signal Process. 58 (2) (2010) 664–678.
[29] Z.-Q. Luo, W.-K. Ma, A.M.-C. So, Y. Ye, S. Zhang, Semidefinite relaxation of quadratic optimization problems, IEEE Signal Process. Mag. 27 (3) (2010) 20–34.
[30] M. Yao, I.A. Hiskens, J.L. Mathieu, Applying Steinmetz circuit design to mitigate voltage unbalance using distributed solar PV, IEEE Milan PowerTech, (2019). Milan, Italy